

An in situ Template Route for Fabricating Metal Chalcogenide Hollow Spherical Assemblies Sonochemically

Shu Xu,^[a] Hui Wang,^[a] Jun-Jie Zhu,^{*[a]} Xin-Quan Xin,^[a] and Hong-Yuan Chen^[a]

Keywords: Sonochemistry / Nanostructures / Self-assembly / Metal chalcogenides / Hollow spheres

An ultrasound-assisted in situ template approach has been developed for fabricating a series of nanoscale metal chalcogenides in the form of well-defined hollow spherical assemblies. These hollow spherical assemblies have well-controlled dimensions and are composed of uniform nanoparticles. Initially, metal hydroxide particles self-assemble into spherical templates generated in situ, and subsequent surface crystal growth leads to hollow spherical structures. Ultrasound irradiation plays a critical role both in the forma-

tion of the intermediate templates and in the crystal-growth process. This approach provides a convenient and efficient one-step pathway to the large-scale fabrication of hollow spherical nanostructures. It also represents a new demonstration of sonochemical effects on the formation and assembly of crystalline particles on the nanometer scale.

(© Wiley-VCH Verlag GmbH & Co. KGaA, 69451 Weinheim, Germany, 2004)

Introduction

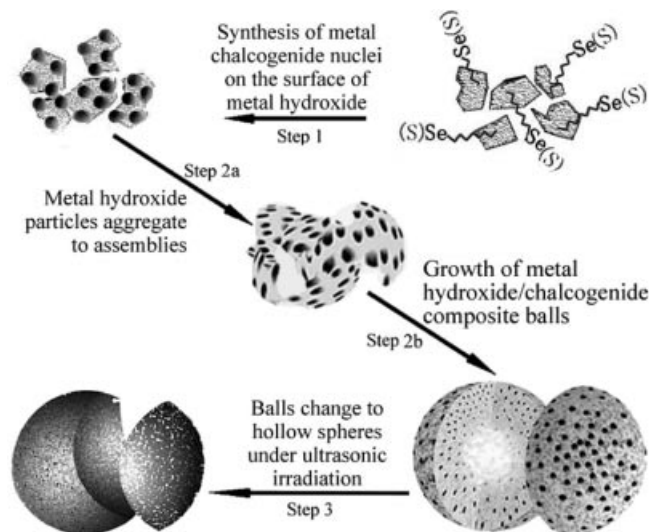
Much attention has been devoted lately to developing methods for preparing, connecting, and assembling semiconductor nanocrystals. The well-ordered assemblies, unlike nanoparticles or single crystals, have new properties suitable for building fine powders or other functional materials. Over the last decades the novel properties and applications of these materials, including mesoporous structures, networks, core-shell spherical materials, and a series of wire- or rod-like assemblies have been exhibited.^[1–9] Especially the assembled hollow spherical materials are important because of their many potential applications in various fields of chemistry, biotechnology, and materials science. For example, they can be used for the transport, controlled storage, and release of chemical and biological products such as drugs, for the protection of biologically active macromolecules, and in the field of catalysis and waste removal.^[10–13] Until now, most methods for the fabrication of inorganic materials with hollow spherical structures were based on a number of well-developed techniques, such as the nozzle reaction system, emulsion/water extraction, layer-by-layer (LBL) self-assembly, and sacrificial core-shell techniques.^[5,14–21]

Currently, the template-directed assembly of nanodimensional materials is arousing increasing interest due to its unique advantages in the control over shape, orientation, and crystal growth. It usually takes three steps to prepare hollow spherical assemblies: first, a colloidal core consisting

of a polymer or some other material is prepared as a template; then, assembly is carried out on the surface of the core to obtain a core-shell structure; finally, the core is removed to form the hollow structure. A widely adopted and quickly developed template method is the LBL self-assembly technique, which is based on the use of electrostatic interactions or hydrogen bonding between alternate layers of materials deposited on a surface. This technique can be applied to the coating of colloids.^[5,18,19] However, only a few hollow spheres of silica, zeolite, and other magnetic materials have been fabricated by using this strategy because of the difficulty in the removal of the template cores. For this reason, we are still trying to find some new methods with the goal of avoiding the disassembly of the shell in the process of removing the cores to produce the final hollow spherical materials, or of even generating hollow spherical structures directly without a core-shell step (Scheme 1).

Ultrasound waves that are intense enough to produce cavitations can drive chemical reactions such as oxidation, reduction, dissolution, decomposition, and polymerization.^[22–33] Ultrasound irradiation has also been employed to prepare a series of polymer core/metal oxide shell particles and a cadmium selenide hollow spherical material.^[9,22,26,34–36] In recent years, the sonochemical method has been proven to be convenient and effective in the fabrication of porous structures. It has been discovered that the ultrasound wave has a strong effect on the congregation and self-assembly of nanoparticles. Gedanken's group has established this procedure as a route to produce some tubular assemblies and a variety of mesoporous oxide materials.^[37–39] The advantage of the application of ultrasound irradiation to the synthesis of mesoporous materials

^[a] State Key Laboratory of Coordination Chemistry, Department of Chemistry, Nanjing University, Nanjing 210093, P. R. China
E-mail: jjzhu@nju.edu.cn



Scheme 1. Proposed mechanism for the synthesis of hollow-sphere materials

is the significant reduction in fabrication time and the possibility to induce the aggregation of nanoparticles into porous structures without destroying the micellar structure. Hence, this method provides an effective surface assembly route for the controllable synthesis of spatially structured materials.

We have extended the sonochemical method to the synthesis of hollow spherical nanostructural materials.^[40] An in situ template route was developed for fabricating a series of metal chalcogenide hollow spherical assemblies in an aqueous system. It is a general approach for fabricating hollow spherical materials directly, which makes it possible to avoid the step of removing the template core.

Results and Discussion

Characterization of Hollow-Sphere Assemblies

Cadmium selenide, cadmium sulfide, and copper sulfide hollow spherical assemblies were prepared. To study the properties and morphology of the products, characterization techniques including powder XRD, TEM, XPS, SAED, UV/Vis absorption and fluorescence spectroscopy were employed.

XRD, XPS Studies, and TEM Observations

The X-ray diffraction patterns for the products are shown in Figure 1. The diffraction peak in pattern (a) indicates that the CdSe particles are crystallized in the pure cubic phase (JCPDS No. 19-191), pattern (b) corresponds to the pure cubic phase CdS (JCPDS No. 75-0581), and pattern (c) belongs to pure CuS crystals (JCPDS No. 03-1090). No peaks of any other impurities were detected, indicating the high purity of the products. According to the Debye–Scherrer equation,^[41] the average sizes of the CdSe,

CdS, and CuS particles were estimated to be about 7 nm, 7 nm, and 10 nm, respectively.

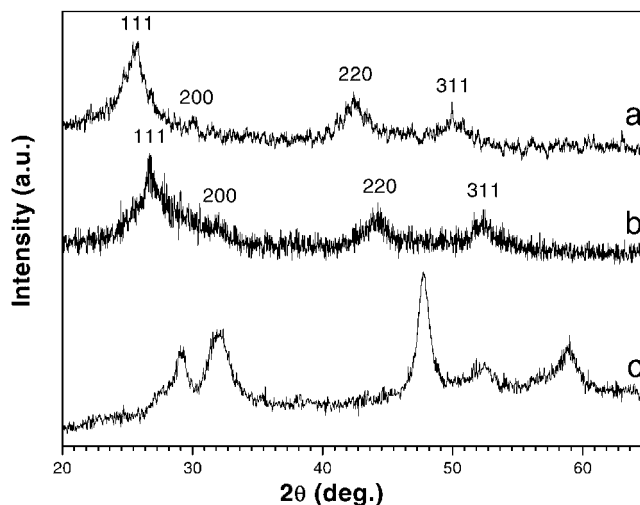


Figure 1. Powder XRD pattern of hollow spherical assemblies: (a) CdSe; (b) CdS; (c) CuS

XPS measurements supply further evidence for the composition and purity of the products. All peaks were calibrated by using C(1s) (284.6 eV) as the reference. The two peaks located at 405.5 eV and 412.3 eV were assigned to Cd(3d). The peaks at 54.5 eV, 162.2 eV, and 932 eV correspond to Se(3d), S(2p), and Cu(2p), respectively. According to the measurements, the ratio Cd/Se is approximately 6:4, which shows that the sample of the CdSe assembly is rich in cadmium at the surface. The measurements also show that the ratio Cd/S is approximately 6:4 and the ratio Cu/S is approximately 1:1.

In the TEM images (Figure 2, a, b), uniform hollow CdSe spheres with an average diameter of 120 nm are observed. These hollow spheres consist of spherical nanoparticles about 5 nm in size. The HRTEM image (Figure 2, c) of a single hollow sphere exhibits the clear crystalline lattice of CdSe particles on the spherical surface and the hollow inside can also be observed clearly. The SAED (Figure 2, d) recorded on a CdSe hollow sphere shows the presence of clear diffraction rings, which correspond to the cubic phase of CdSe with polycrystalline nature. In Figure 3, uniform hollow CdS spheres with an average diameter of 120 nm are observed. The surface structure of the CdS spheres is the same as that of the hollow CdSe spheres assembled from nanoparticles about 5 nm in size. Figure 4 shows the TEM image of the CuS hollow spheres with diameters ranging from 150 to 300 nm. These spheres are made up of CuS nanoparticles about 8 nm in size. The shell of the CuS sphere is thinner than that of the hollow CdSe and CdS spheres, so the hollow space inside is very distinct. The TEM images confirm that all the spheres for all three compounds are hollow.

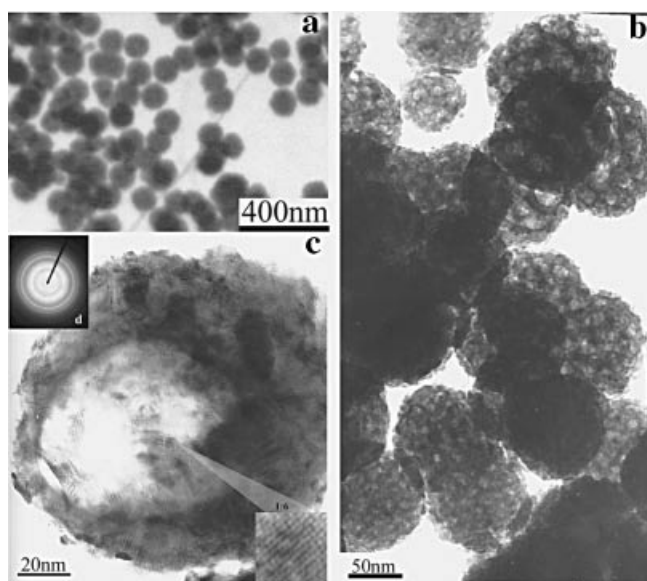


Figure 2. TEM and HRTEM images of the CdSe assemblies in the presence of ammonia after sonication for 30 min (concentration of NH_3 : 0.8 mol/L): (a, b) TEM images of the product, (c) HRTEM image of an individual CdSe hollow-spherical assembly, (d) [inset in (c)] SAED pattern recorded on the hollow sphere shown in (c)

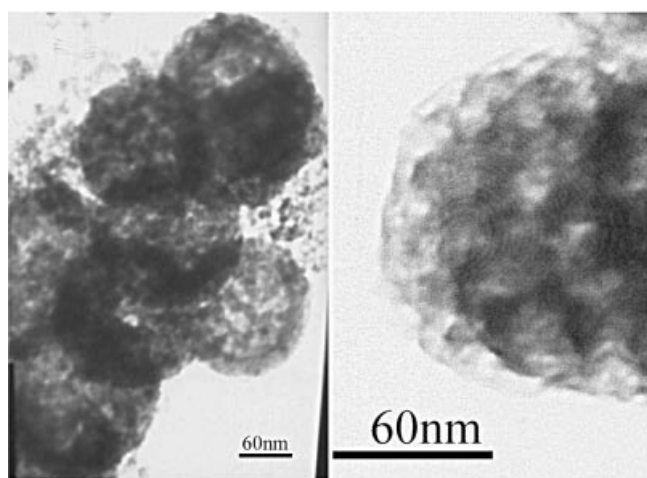


Figure 3. TEM images of the CdS assemblies in the presence of ammonia after sonication for 30 min (concentration of NH_3 : 0.8 mol/L)

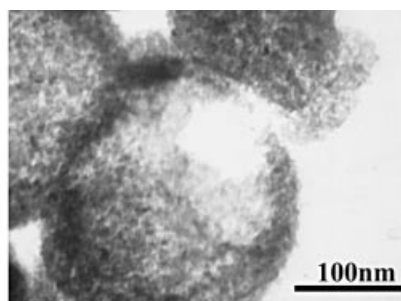
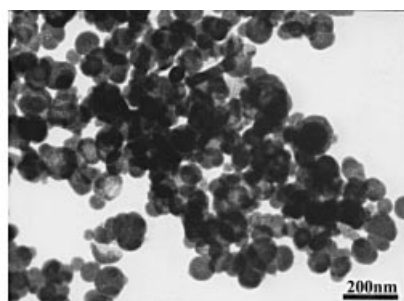


Figure 4. TEM images of the CuS assemblies in the presence of TEA after sonication for 30 min (concentration of TEA: 0.8 mol/L)

Optical Characterization

The UV/Vis absorbance spectra of the prepared hollow spherical materials were measured and their correlative optical band gaps were calculated according to the following Equation, where A is a constant, α is the absorption coefficient, and $m = 3$ for a direct and $m = 1$ for an indirect transition.^[42]

$$\alpha(\nu) = A \cdot [h\nu / (2 - E_g)]^{m/2}$$

The CdSe assembly has its absorbance peak at 350 nm. Its direct band gap is calculated to be 2.7 eV, which is much larger than the reported value for bulk CdSe ($E_g = 1.7$ eV).^[43] This band-gap value, which indicates the quantum size effect of this sample, equals that of the 7 nm quantum CdSe nanoparticles prepared. It offers further evidence that these spherical assemblies are made up of smaller nanoparticles. The direct band gap of the hollow CdS assemblies is calculated to be 2.11 eV. The equation with $m = 1$ is used for the indirect transition to the copper sulfide nanoparticles, since copper sulfide is a typical indirect semiconductor.^[44] The calculated band gap of this CuS assembly is 2.02 eV, which equals that of 8 nm CuS nanoparticles.

We also investigated the fluorescent absorbance spectra of the prepared materials and compared them with those of the dispersed particles. The excitation and emission wavelengths of the hollow CdSe spheres were 485 nm and 730 nm, respectively; the fluorescence spectrum was the same as that of dispersed 5 nm CdSe nanoparticles. The emission peak of CdS was at 570 nm when an excitation wavelength of 430 nm was selected. The CuS sphere had a strong emission peak at 362 nm when the excitation wavelength was 220 nm.

Discussion of the Reaction Procedure

A study of the reaction processes showed that metal hydroxide was an in situ template in the reaction and directed the formation of hollow spherical structures. We propose a probable reaction mechanism to explain the formation of hollow spherical materials in accordance with our experimental results. The effect of ultrasound irradiation, release rate of Se^{2-} and S^{2-} ions, pH value and ligands on the reaction were also investigated.

Microscopic Monitoring of the Reaction Process

The structures of the assemblies at various stages of the growth process were characterized using TEM. We collected the products every 5 min during the reaction. The precursor, the intermediate structure formed during the sonochemical reaction, and the final structure are shown in Figure 5. These TEM images indicate the tendency to form a hollow spherical structure from the metal hydroxide particles. To begin with, ammonia or triethylamine was added to an aqueous solution of metal ions to form a metal hydroxide colloidal solution. The metal hydroxide particles were made up of many very irregular slices and some blocks, as shown in Figure 5 (a). Initially, the metal hydroxide particles reacted with selenium or sulfur ions, giving rise to metal chalcogenide nanoparticles on their surface, and formed metal hydroxide/chalcogenide composites. In the medial stage (Figure 5, b), we could observe that some slices and blocks were interconnected and enwrapped to form balls or multilayered spheres. At the final stage (Figure 5, c), the balls had grown into regular hollow spheres. Furthermore, when the ultrasound intensity was lower than 15 W/cm^2 , the products were inclined to form irregular hollow spheres or balls, whereas an intensity higher than 30 W/cm^2 lead to the formation of dispersed particles. All the experiments showed that ultrasound waves had a critical effect on the fabrication of the special structures.

We also investigated some contrastive experiments and compared the morphology of the products in different stages of the reaction process with that in the process of fabricating hollow spheres. In the thermal process, in which sonication was replaced by heating and stirring, the metal hydroxide and chalcogenide particles continuously congregated to form large irregular assemblies instead of spheres. These assemblies were also composed of 7–10 nm metal chalcogenide nanoparticles. On the other hand, when metal hydroxide particles alone were sonicated, they formed rod-like crystals or assemblies. When metal hydroxide particles alone were heated, their congregation was much slower and

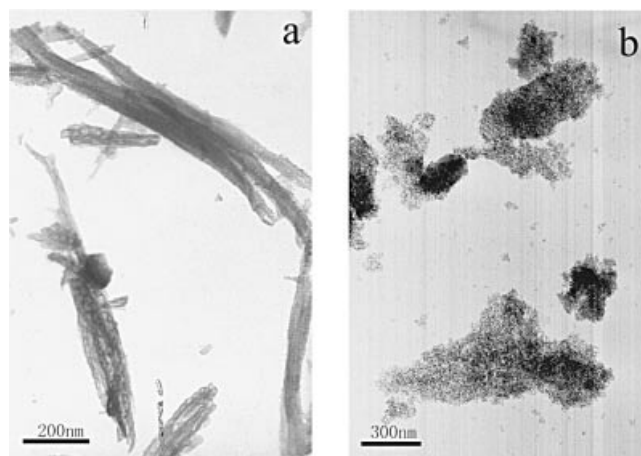


Figure 6. TEM images: (a) cadmium hydroxide nanorods prepared (cadmium hydroxide was sonicated for 30 min in the presence of ammonia); (b) cadmium sulfide particles prepared by the thermal process (cadmium hydroxide reacted with Na_2SeSO_3 at 90°C for 30 min in the presence of ammonia)

more irregular. Figure 6 exhibits the morphology of a sample of cadmium hydroxide sonicated for 30 min and a cadmium sulfide aggregate prepared by the thermal process. None of these reactions produced a sphere-like structure.

Probable Reaction Mechanism

In a typical reaction, ultrasound irradiation induces the assembly of the metal hydroxide particles into both balls and hollow spherical structures and the growth of cadmium chalcogenide crystals on the template surface.

The elevated temperatures and pressures inside the collapsing bubbles cause water to vaporize and to further pyrolyze into H^\cdot and OH^\cdot radicals during an aqueous sonochemical process.^[22] The H^\cdot and OH^\cdot radicals can react with sodium selenosulfate and thiourea to release Se^{2-} and S^{2-} . The dangling bonds on the surface of the metal hydroxide particles provide some active spots for the formation of me-

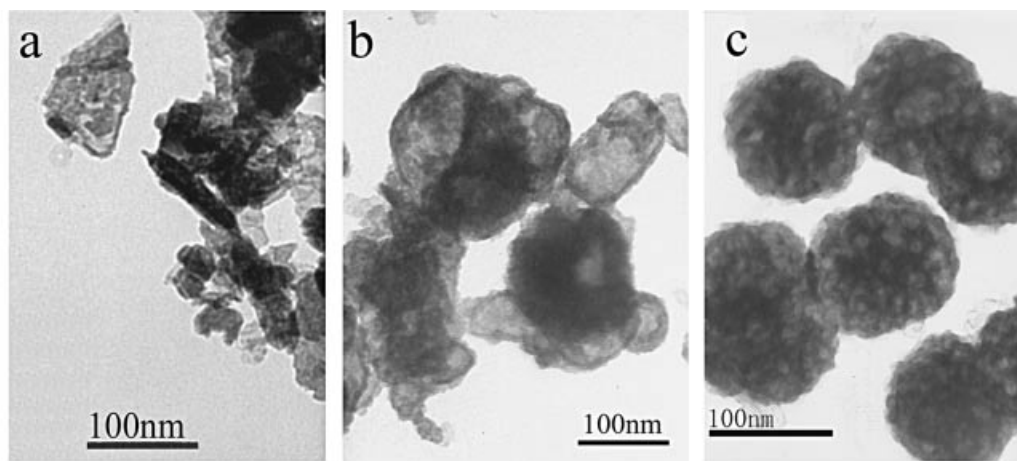
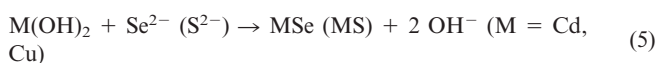
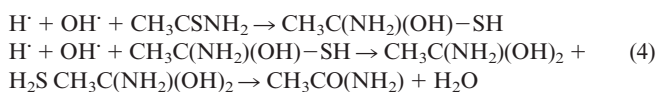
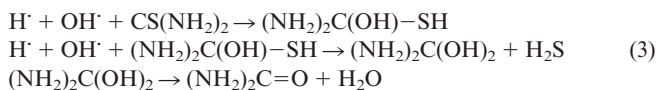
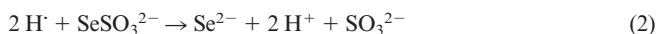


Figure 5. TEM images of the products at different stages of fabricating CdSe hollow spheres (sonic intensity is 20 W/cm^2): (a) cadmium hydroxide particles at the initial stage (immediately after precipitation); (b) after 15 min reaction; (c) after 30 min reaction

tal chalcogenide nuclei. The probable reaction sequence for the sonochemical formation of the metal chalcogenide nanoparticles can be summarized as shown in Equations (1)–(6).



The freshly born nuclei will grow into large particles until they become stable finally. It is well known that the Gibbs free energy of the surface of small-sized nanoparticles is usually very high due to the large surface/volume ratio and the existence of dangling bonds on the surface. These small particles have the tendency to aggregate, to decrease the Gibbs free energy of the surface and to make the surface state stable. In most cases, the smaller nanoparticles result in more easy aggregation. In our experiments, the particles grown on the metal hydroxide were also inclined to conglomeration. The kinetics of the thermal process enables the formation of Se and S ions and the growth of metal chalcogenide nanoparticles, which induce congregation. Since this kind of congregation is not directional assembly, the final product consists of big irregular particles as shown in part b of Figure 6.

On the other hand, in the sonication process, cavitation resulting in bubble collapse will launch shock waves out into the liquid. The strength of the waves can even result in the breakage of the bonds in the polymer chain. When these shock waves pass over metal hydroxide and metal oxide particles, they can also cause the rapid impact of the liquid on the surface of the particles and promote the rupture of the bonds.^[25] Ultrasound studies have indicated that a large number of dangling bonds and defects will appear especially at the edge of sheetlike particles as a result of the impingements of the microjets created by ultrasonic waves.^[22,45] Gedanken's group has produced a kind of tubular titania assembly using this mechanism.^[39] If only metal hydroxide particles were under sonication, the many dangling Cd–O–Cd bonds on the edges of the sheetlike particles would connect to form a layer-like structure which continuously rolls into rods or tubes as the structure observed in Figure 6 (a).

However, in our system, the metal hydroxide particles were not merely assembled through the dangling Cd–O–Cd bonds or the metal chalcogenide nuclei on the surface. Once the chalcogenide nuclei were formed on the surface of the hydroxide particles, the effect resulted in the assembly both on the edge by the connection of the dangling Cd–O–Cd bonds, and on the surface by the congregation of the chalcogenide nanoparticles. The two kinds of assembly lead to intermediate products with ball-like or multilayered hollow-spherical structures, as observed in the TEM images (see b in Figure 3).

After the formation of the intermediate structure, the growth of the metal chalcogenide particles only on the surface of the metal hydroxide/chalcogenide composite spheres continually consumed the inner metal hydroxide. These freshly born nuclei grew into large particles until they finally became stable.^[46] The product was a regular hollow sphere. The metal chalcogenide particles thus formed were held together by van der Waals forces. Since these forces are not very strong, the rapid impact of the liquid would promote the dispersion of the assemblies, which would crack into small particles and disperse further in the presence of the strong ultrasound shock wave. Hence, a high sonic intensity could not be used in the experiments. When the aggregation and dispersion were balanced, the metal hydroxides could aggregate to form the desired assemblies; then the reaction could be carried out to fabricate the hollow-sphere structures described in Equations (5) and (6). At a sonic intensity of 20 W/cm², a good balance was observed, and an appropriate growth rate could be obtained.

Effect of the Release Rate of Chalcogen Ions

In our further studies, we determined that the growth rate of metal chalcogenide nuclei had a strong effect on the fabrication process. This effect depended on the release rate of Se²⁻ and S²⁻. With a high release rate, many metal chalcogenide nuclei and particles would grow on the surface of the metal hydroxide particles before their assembly. In this case, the number of the remaining metal hydroxide particles was not enough for crystal growth on the surface to form hollow structures and aggregation neutralized the dispersive effect of ultrasound. The result was ball-like metal chalcogenide aggregation instead of hollow spherical assemblies. In contrast, a low release rate would make the dispersive effect of ultrasound so strong that the particles would break away from the surface. This resulted in incompact hollow spheres or dispersed particles.

In the presence of ultrasonic irradiation, the release rates of Se²⁻ and S²⁻ from different selenium and sulfur sources are different. Our study on the growth of CdS spheres proved the importance of selecting the appropriate sulfur source. When thiourea was the sulfur source, the release rate of S ions was slow, and the white turbid suspension began to turn yellow after 10 min of reaction. After 30 min of reaction, the product consisted almost completely of dispersed particles, and only a few hollow spheres were observed. Alternatively, when thioacetamide was selected as

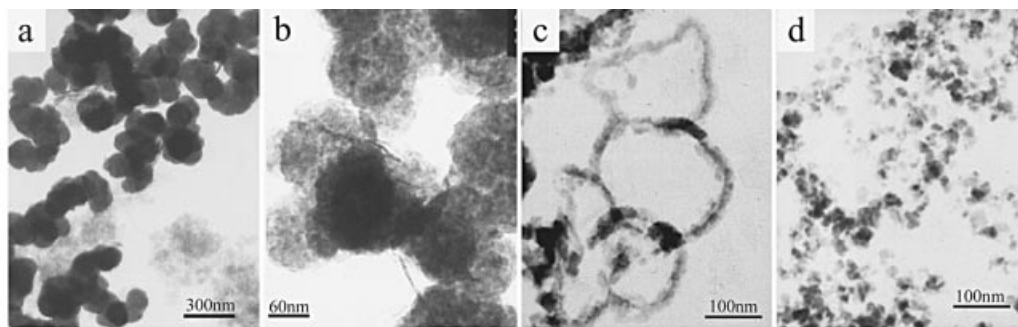


Figure 7. TEM images of the CdS particles obtained with different thiourea/thioacetamide ratios as the sulfur source (sonic intensity: 20 W/cm²; sonication time: 30 min): (a) thioacetamide as the sulfur source; (b) with a 1:1 ratio of thiourea/thioacetamide; (c) with a 4:1 ratio of thiourea/thioacetamide; (d) thiourea as the sulfur source

the sulfur source, the release rate of S²⁻ was quick enough to form the yellow turbidity immediately. After 30 min of reaction, all of the product was ball-like and no hollow spherical structure was observed. Only when the ratio thiourea/thioacetamide was in an appropriate range would the hollow spherical structure be fabricated. The TEM images in Figure 7 show a series of structures ranging from ball, hollow sphere, circle-like to dispersed particles. It seemed that the dispersed particles were decomposed from the circles. The relation between the structures was strong evidence for the dispersive effect of sonication. In the preparation of cadmium selenide, the experimental results showed that the release rate of Se²⁻ from sodium selenosulfate was acceptable in the fabrication of CdSe hollow spheres.

Effect of the Ligands on the Reaction

Se²⁻ and S²⁻ need to be released in an alkaline environment; otherwise the release rate will be too slow to fabricate the assemblies. In our experiments, the pH value of the reaction system was kept at about 10 by adjusting the ligands and the reactants in the solution. The ligands in the solution were also important in the control of both the formation of metal chalcogenide nuclei and the crystal-growth rate. According to our experiments, in the absence of the ligands or with ligands having weak complexing ability, the products would be dispersed particles or irregular assemblies. Some unidentate and chelating ligands with strong complexing capability and steric effects would strongly decrease the growth of the nanoparticles and lead to monodispersed particles or even prevent the metal ions from combining with the Se²⁻ and S²⁻ ions. This observation proved the protection effect of the ligands. Through the complexing action between metal ions and ligands that lead to the formation of the complexes, the ligands could protect the metal ions from reacting with Se²⁻ and S²⁻ directly and provided a stable reaction rate. Here we selected ammonia and tetraethylammonium (TEA) as the ligands because they had a moderate complexing ability for the metal ions in the alkaline environment. In addition, the concentration of the ligands had to be limited to a certain range; otherwise the ligands in excess would dissolve all the metal hydroxide particles. Actually, in the reaction system

the ligands were adsorbed on the surface of the metal hydroxide stoichiometrically. The steric effect enhanced the stability of the surface structure and controlled the rate of combination of Se²⁻ and S²⁻ with the metal ions.

Conclusion

A general sonochemical approach for the fabrication of hollow spherical assemblies composed of metal chalcogenide nanoparticles has been successfully established. In this reaction, we make the best use of the balance between the conglomeration of the particles and the dispersive effect of ultrasound to direct the growth of the assemblies. As we have demonstrated in this article, the effect of ultrasound on the metal hydroxide balls directs the formation of the in situ template, and the growth on the surface leads to the fabrication of the final hollow-sphere assemblies. The sonochemical method provides a mild, energy-efficient, and environment-friendly approach to hollow-sphere assemblies of nanodimensional metal chalcogenides. Furthermore, a major advantage is that it circumvents the disassembly of the shell in the process of removing the cores and produces the hollow metal chalcogenide spheres conveniently. It promises to be useful in the fabrication of other hollow assemblies composed of metal, alloy, oxide, and similar nanoparticles.

Experimental Section

General: All reagents used were of analytical purity. Na₂SeSO₃ solution (0.2 M) was prepared by stirring Se (0.2 M) and Na₂SO₃ (0.5 M) at about 70 °C for 24 h. The XRD patterns were recorded with a Shimadzu XD-3 A X-ray diffractometer (Cu-K_α radiation, λ = 0.15418 nm). The TEM and SAED examinations were carried out with a JEOL JEM-200CX transmission electron microscope, with an accelerating voltage of 200 kV. The surface of the products was studied by X-ray photoelectron spectroscopy with an ESCALAB MK II X-ray photoelectron spectrometer, taking nonmonochromatized Mg-K_α X-ray as the excitation source and choosing C(1s) (284.6 eV) as the reference line. A Ruili 1200 spectrophotometer (Peking Analytical Instrument Co.) was used to record the UV/Vis absorption spectra of the CdSe, CdS and CuS assemblies.

Preparation of Hollow CdSe Spheres: CdCl₂ (0.5 g) was dissolved in distilled water (50 mL), and then ammonia (5 mL, 30% NH₃) or TEA (11 mL) was added. A white colloid appeared immediately in the solution. This solution, Na₂SeSO₃ (10 mL, 0.2 M), and the amount of distilled water to make the total volume 100 mL were transferred into a 150-mL round-bottom flask. This mixture was irradiated with a high-intensity ultrasonic horn (Xinzhi C, China, Ti horn, 20 kHz, 60 W/cm²) under ambient conditions in air for 30 min, and a dark red precipitate was obtained. After being cooled to room temperature, the precipitate was centrifuged, washed with distilled water followed by acetone, and then dried in air.

Preparation of Hollow CdS Spheres: Thiourea (0.15 g) and thioacetamide (0.05 g) were dissolved in distilled water (50 mL) and mixed with the CdCl₂/ammonia colloid solution. The final product was a yellow precipitate.

Preparation of Hollow CuS Spheres: CuSO₄ (0.35 g) was dissolved in distilled water (50 mL), and then TEA (10 mL) was added. A green colloid was observed. After adding thiourea (0.15 g), the product was a black precipitate.

Preparation of Dispersed Nanoparticles: The reaction for preparing CdSe and CdS nanoparticles was the same as that for hollow spheres, with the difference that the TEA ligand was used in excess. No ligand was used in the reaction for preparing CuS nanoparticles.

Acknowledgments

This work was supported by the National Natural Science Foundation of China (No. 20325516, 90206037).

- [1] *Characterization of Nanophase Materials* (Ed.: Z. L. Wang), Wiley-VCH, Weinheim, **2000**.
- [2] W. Scharfl, *Adv. Mater.* **2000**, *12*, 1899–1908.
- [3] W. U. Huynh, J. J. Dittmer, A. P. Alivisatos, *Science* **2002**, *295*, 2425–2427.
- [4] Z. Y. Tang, N. A. Kotov, M. Giersig, *Science* **2002**, *297*, 237–240.
- [5] F. Caruso, R. A. Caruso, H. Mohwald, *Science* **1998**, *282*, 1111–1114.
- [6] M. Brust, C. J. Kiely, *Colloids Surf., A* **2002**, *202*, 175–186.
- [7] S. A. Davis, M. Breulmann, K. H. Rhodes, B. Zhang, S. Mann, *Chem. Mater.* **2001**, *13*, 3218–3226.
- [8] M. deWild, S. Berner, H. Suzuki, L. Ramoino, A. Baratoff, T. A. Jung, *Chimia* **2002**, *56*, 500–505.
- [9] D. N. Srivastava, N. Perkas, G. A. Seisenbaeva, Y. Koltypin, V. G. Kessler, A. Gedanken, *Ultrasound. Sonochem.* **2003**, *10*, 1–9.
- [10] D. L. Wilcox, M. Berg, T. Bernat, D. Kellerman, J. K. Cochran, *Hollow and Solid Spheres and Microspheres: Science and Technology Associated with Their Fabrication and Application, Materials Research Society Proceedings*, Materials Research Society, Pittsburgh, **1995**, vol. 372.
- [11] H. Y. Huang, E. E. Remsen, *J. Am. Chem. Soc.* **1999**, *121*, 3805–3806.
- [12] T. K. Mandal, M. S. Fleming, D. R. Walt, *Chem. Mater.* **2000**, *12*, 3481–3487.
- [13] F. Caruso, X. Y. Shi, R. A. Caruso, A. Susa, *Adv. Mater.* **2001**, *13*, 740–744.
- [14] J. K. Cochran, *Curr. Opin. Solid State Mater. Sci.* **1998**, *3*, 474.
- [15] G. Decher, *Science* **1997**, *277*, 1232–1237.
- [16] Z. Y. Zhong, Y. D. Yin, B. Gates, Y. N. Xia, *Adv. Mater.* **2000**, *12*, 206–209.
- [17] H. P. Lin, Y. R. Cheng, C. Y. Mou, *Chem. Mater.* **1998**, *10*, 3772–3776.
- [18] F. Caruso, *Chem. Eur. J.* **2000**, *6*, 413–419.
- [19] X. D. Wang, W. L. Yang, Y. Tang, Y. J. Wang, S. K. Fu, Z. Gao, *Chem. Commun.* **2000**, 2161–2162.
- [20] J. X. Huang, Y. Xie, B. Li, Y. Liu, Y. T. Qian, S. Y. Zhang, *Adv. Mater.* **2000**, *12*, 808–811.
- [21] X. C. Jiang, Y. Xie, J. Y. Lu, L. Zhu, W. He, X. M. Liu, *Can. J. Chem.* **2002**, *80*, 263–268.
- [22] K. S. Suslick, *Ultrasound: Its Chemical, Physical, and Biological Effects*, VCH Verlagsgesellschaft, Weinheim, **1988**.
- [23] K. S. Suslick, D. A. Hammerton, R. E. Cline, *J. Am. Chem. Soc.* **1986**, *108*, 5641–5642.
- [24] K. S. Suslick, S. B. Choe, A. A. Cichowlas, M. W. Grinstaff, *Nature* **1991**, *353*, 414–416.
- [25] T. Hyeon, M. Fang, K. S. Suslick, *J. Am. Chem. Soc.* **1996**, *118*, 5492–5493.
- [26] K. S. Suslick, G. J. Price, *Ann. Rev. Mater. Sci.* **1999**, *29*, 295–326.
- [27] N. A. Dhas, A. Gedanken, *J. Phys. Chem. B* **1997**, *101*, 9495–9503.
- [28] R. V. Kumar, Y. Diamant, A. Gedanken, *Chem. Mater.* **2000**, *12*, 2301.
- [29] J. J. Zhu, Y. Koltypin, A. Gedanken, *Chem. Mater.* **2000**, *12*, 73–78.
- [30] R. Kerner, O. Palchik, A. Gedanken, *Chem. Mater.* **2001**, *13*, 1413–1419.
- [31] H. Wang, J. J. Zhu, J. M. Zhu, H. Y. Chen, *J. Phys. Chem. B* **2002**, *106*, 3848–3854.
- [32] H. Wang, J. J. Zhu, J. M. Zhu, X. H. Liao, S. Xu, T. Ding, H. Y. Chen, *Phys. Chem. Chem. Phys.* **2002**, *4*, 3794–3799.
- [33] J. J. Zhu, H. Wang, S. Xu, H. Y. Chen, *Langmuir* **2002**, *18*, 3306–3310.
- [34] O. Palchik, G. Kataby, Y. Mastai, A. Gedanken, *Adv. Mater.* **1999**, *11*, 1289–1292.
- [35] M. L. Breen, A. D. Dinsmore, R. H. Pink, S. B. Qadri, B. R. Ratna, *Langmuir* **2001**, *17*, 903–907.
- [36] X. W. Zheng, Y. Xie, L. Y. Zhu, X. C. Jiang, A. H. Yan, *Ultrasound. Sonochem.* **2002**, *9*, 311–316.
- [37] A. Gedanken, X. H. Tang, Y. Q. Wang, N. Perkas, Y. Koltypin, M. V. Landau, L. Vradman, M. Herskowitz, *Chem. Eur. J.* **2001**, *7*, 4546–4552.
- [38] Y. Q. Wang, L. X. Yin, A. Gedanken, *Ultrasound. Sonochem.* **2002**, *9*, 285–290.
- [39] Y. C. Zhu, H. L. Li, Y. Koltypin, Y. R. Hacohen, A. Gedanken, *Chem. Commun.* **2001**, 2616–2617.
- [40] J. J. Zhu, S. Xu, H. Wang, J. M. Zhu, H. Y. Chen, *Adv. Mater.* **2003**, *15*, 156–160.
- [41] *X-ray Diffraction Procedures* (Eds.: H. Klug, L. Alexander), Wiley, New York, **1962**.
- [42] S. Tsunekawa, T. Fukuda, A. J. Kasuya, *Appl. Phys.* **2000**, *87*, 1318–1321.
- [43] K. R. Patil, D. V. Paranjape, S. D. Sathaye, A. Mitra, S. R. Padalkar, A. B. Mandale, *Mater. Lett.* **2000**, *46*, 81–85.
- [44] L. Reijnen, B. Meester, A. Goossens, J. Schoonman, *J. Mater. Sci. Eng. C* **2002**, *19*, 311–314.
- [45] S. Andersson, A. D. Wadsley, *Acta Crystallogr.* **1961**, *14*, 1245–1249.
- [46] W. Chen, Z. G. Wang, Z. J. Lin, L. Y. Lin, *J. Appl. Phys.* **1997**, *82*, 3111–3115.

Received March 26, 2004

Early View Article

Published Online October 7, 2004